Competitive Te-Te and C-Te Bond Cleavage on the Oxidative Addition of Aryl and Alkyl Ditellurides to Pt(0) Centers †

Minna M. Karjalainen,[a] Torben Wiegand,[b] J. Mikko Rautiainen,[a,c] Andreas Wagner,[a,b] Helmar Görls,[b] Wolfgang Weigand,[b] Raija Oilunkaniemi,[a] and Risto S. Laitinen*,[a]

The oxidative addition reaction of ditellurides R_2Te_2 [R = ^{n}Bu, Ph, Th (2-thienyl, C_4H_3S)] to [Pt(η^2-nb)(*dppn*)] (nb = norbornene, *dppn* = 1,2-bis(diphenylphosphino)naphthalene) was found to afford [Pt(TeR)$_2$(*dppn*)] [R = ^{n}Bu (**1**), Ph (**2**), Th (**3**)] and [Pt(TeR)(R)(*dppn*)] [R = Ph (**4**), Th (**5**)] as a result of the cleavage of the Te-Te or C-Te bond, respectively. The reactions and the product distributions were monitored by $^{31}P\{^1H\}$ NMR spectroscopy. The spectral interpretation was assisted by the high-yield preparation of [Pt(TePh)$_2$(*dppn*)] (**2**) and [Pt(TeTh)$_2$(*dppn*)] (**3**) by ligand echange reactions from [PtCl$_2$(*dppn*)], and by the crystal structure determinations and spectral characterizations of **2** and **3**. Two series of reactions were carried out both at room temperature and at -80 °C. One involved the addition of the toluene solution of R_2Te_2 to that of [Pt(η^2-nb)(*dppn*)], and the other the addition of [Pt(η^2-nb)(*dppn*)] solution to the R_2Te_2 solution. The oxidative addition of ^{n}Bu$_2$Te$_2$ to [Pt(η^2-nb)(*dppn*)] yielded solely [Pt(Te^{n}Bu)$_2$(*dppn*)]. In case of Ph_2Te_2 and Th_2Te_2, the reaction of equimolar amounts of ditelluride and [Pt(η^2-nb)(*dppn*)] afforded only [Pt(TeR)(R)(*dppn*)] (R = Ph, Th), but when an excess of R_2Te_2 was used, the addition of [Pt(η^2-nb)(*dppn*)] to the ditelluride resulted in the formation of a mixture of [Pt(TeR)$_2$(*dppn*)] and [Pt(TeR)(R)(*dppn*)] with the latter the main component. An excess of R_2Te_2 and the lowering of the temperature favoured the formation of [Pt(TeR)$_2$(*dppn*)]. The reaction energetics in toluene was calculated at revPBE GGA DFT / TZVP(f) level of theory. The increase of the electron withdrawing nature of the organic substituent rendered [Pt(TeR)(R)(*dppn*)] increasingly stable with respect to [Pt(TeR)$_2$(*dppn*)]. The computation of the energy profiles of the likely pathways of the oxidative addition indicated that concurrent formation of [Pt(TeR)$_2$(*dppn*)] and [Pt(TeR)(R)(*dppn*)] (R = Ph, Th) may be more likely than the formation of the latter due to the decomposition of the former. This was verified experimentally by stirring pure [Pt(TeR)$_2$(*dppn*)] in toluene for a prolonged time at room tempertature. No decomposition was observed.

Introduction

The oxidative addition of dichalcogenides to Pt(0) or Pd(0) complexes is considered to be an important step in the catalytic addition of dichalcogenides to alkenes or alkynes and finds use in regioselective and stereospecific organic synthetic chemistry (for recent comprehensive reviews, see ref. 1). The initial step in the catalysis is considered to involve the oxidative addition of dichalcogenides to Pd(0) or Pt(0) centers.[2] In case of organic disulfides or diselenides it generally leads to the cleavage of the sulfur-sulfur or selenium-selenium bonds and the formation of chalcogenolato complexes, the formation and coordination chemistry of which have been reviewed on several occasions.[3] In case of ditellurides, the cleavage of the tellurium-carbon bond may also take place in addition to that of the tellurium-tellurium bond.[3d,4] There are indications that in case of aliphatic ditellurides, only Te-Te bond cleavage takes place,[4a,5] but the C-Te cleavage is also observed in case of diaryl ditellurides.[4b,c] The competitive activation between the Te-Te and C-Te bonds has been considered to be one of the reasons, why the catalytic properties of the tellurolato complexes are inferior to those of thiolato and selenolato complexes.[1c,5a-c] The regioselective C-Te bond cleavage upon oxidative addition has been discussed considering the reactions of Ph_2Te [6] and $PhTeMMe_3$ (M = Si, Ge, Sn) [7] with tetrakis(triorganophosphane)platinum.

The kinetics and mechanism of the oxidative addition of dichalcogenides to Pd(0) and Pt(0) complexes have been reviewed recently.[8] DFT calculations on reaction pathways and trends in controlling factors of reaction between R_2E_2 (E = S, Se, Te; R = H, Me) and [M(PR'$_3$)$_2$] (M = Pd, Pt; R' = H, Me) have also been reported.[9]

In this contribution, we revisit the factors governing the competitive Te-Te or C-Te bond cleavage upon oxidative addition of organic ditellurides to Pt(0) center by carrying out reactions of [Pt(η^2-nb)(*dppn*)] [nb = norbornene, *dppn* = bis(diphenylphosphino)naphthalene] with R_2Te_2 [R = ^{n}Bu, Ph, Th (thienyl = 2-C_4H_3S)] and varying carefully the reaction parameters. Whereas, the oxidative addition of ^{n}Bu$_2$Te$_2$ to [Pt(η^2-nb)(*dppn*)] led to the sole formation of [Pt(Te^{n}Bu)$_2$(*dppn*)] (**1**), the reactions of Ph_2Te_2 and Th_2Te_2 resulted in mixtures containing [Pt(TePh)$_2$(*dppn*)] (**2**) and [Pt(TePh)(Ph)(*dppn*)] (**4**), and [Pt(TeTh)$_2$(*dppn*)] (**3**) and [Pt(TeTh)(Th)(*dppn*)] (**5**), respectively. The fundamental question is, whether complexes **4** and **5** were formed concurrently with complexes **2** and **3**, respectively, or sequentially as a result of the decomposition of the complexes **2** and **3**. The reactions were monitored using ^{31}P NMR spectroscopy. The determination of the crystal structures of **2**-**5** and their chemical shifts were utilized in the assignment of the NMR spectra of the reaction mixtures. The experimental

[a] *Laboratory of Inorganic Chemistry, University of Oulu, P. O. Box 3000, FI-90014 University of Oulu, Finland. Email. risto.laitinen@oulu.fi.*
[b] *Institut für Anorganische und Analytische Chemie, Humbold-Str. 8, 07743, Friedrich-Schiller-Universität Jena, Germany*
[c] *Present address: Department of Chemistry, University of Jyväskylä, P.O. Box 35, FI-40014 University of Jyväskylä, Finland.*

† Electronic Supplementary Information (ESI) available: Crystal data and details of structure determination and selected bond parameters of **2**-**5**, CCDC 1522462-1522465, Definition of the angle of distortion. Energy profile of Th_2Te_2 + [Pt((η^2-nb)(*dppn*)]. $^{31}P\{^1H\}$ NMR spectrum of [Pt(TeTh)$_2$(*dppn*)].

observations were complemented with DFT calculations on the energy profiles of the reaction pathways.

Experimental

General

All reactions and manipulations of air- and moisture-sensitive reagents were carried out under an inert argon atmosphere by using Schlenk techniques. Ph_2Te_2 (Aldrich) was used as supplied, and Th_2Te_2,[10] $^nBu_2Te_2$,[11] [$PtCl_2$(*dppn*)],[12] and [Pt(η²-nb)(*dppn*)] [13] were prepared according to the literature procedures. THF, toluene, and hexane were dried by distillation over Na/benzophenone prior to use.

NMR Spectcroscopy

The $^{31}P\{^1H\}$, $^{125}Te\{^1H\}$, and $^{195}Pt\{^1H\}$ NMR spectra were recorded on a Bruker Avance III spectrometer in THF operating at 161.98, 126.27, and 85.60 MHz, respectively. Orthophosphoric acid (85 %), a saturated D_2O solution of H_6TeO_6, and the D_2O solution of $[PtCl_4]^{2-}$ were used as external standards. The ^{31}P chemical shifts are reported relative to the external standard, the ^{125}Te chemical shifts relative to neat Me_2Te {$\delta(Me_2Te) = \delta(H_6TeO_6) + 710.9$] [14]}, and ^{195}Pt chemical shifts relative to $[PtCl_6]^{2-}$ {$[\delta(PtCl_6^{2-}) = \delta(PtCl_4^{2-}) - 1624]$ [15]}. The spectra were recorded unlocked.

X-ray Crystallography

Diffraction data for compounds **2**·3C_7H_8 and **3**-**5** were collected on a Nonius Kappa CCD diffractometer using graphite monochromated Mo Kα radiation (λ = 0.71073 Å). Crystal data and the details of the structure determinations are presented in ESI (see Table 1S). The structures were solved by direct methods using SHELXS-2013 and refined using SHELXL-2013.[16] After the full-matrix least-squares refinement of the non-hydrogen atoms with anisotropic thermal parameters, the hydrogen atoms were placed in calculated positions. In the final refinement, the calculated hydrogen atoms were riding with the carbon atom they were bonded to. The isotropic thermal parameters of the aromatic hydrogen atoms were fixed at 1.2, and those of aliphatic hydrogen atoms at 1.5 times to that of the corresponding carbon atom. The scattering factors for the neutral atoms were those incorporated with the program.

The solvent molecule in **3**·C_7H_8 turned out to be disordered and the toluene molecule assumed two orientations. The refinement of the site occupation factors was made by constraining the thermal parameters of each atom to be equal. The refinement resulted in the s.o.f. values of *ca.* 25 % for every atom. In the final refinement, the site occupation factors of all atoms in the solvent were therefore fixed at 25 %.

Preparation of [Pt(Te^{n}Bu)$_2$(*dppn*)] (1)

$^nBu_2Te_2$ (0.045 g, 0.122 mmol) was added to [Pt(η²-nb)(*dppn*)] (0.095 g, 0.121 mmol), which was dissolved in 5 ml of toluene. The solution was stirred for 5 minutes and concentrated upon evaporation of the solvent. The precipitation was filtered and the orange solid was washed with *n*-hexane and dried. Yield 0.077 g, 60 %. Anal. Calcd. (%) for $PtTe_2P_2C_{42}H_{44}$: C, 47.54; H 4.18. Found: C, 47.68; H, 4.07.

Preparation of [Pt(TePh)$_2$(*dppn*)] (2)

$NaBH_4$ (0.058 g, 1.54 mmol) and methanol (5 ml) was added to a solution of Ph_2Te_2 (0.300 g, 0.733 mmol) in toluene (10 ml) and the solution was stirred for *ca*. 15 min. 4 ml of this solution (0.391 mmol $PhTe^-$) was added to a slurry of [$PtCl_2$(*dppn*)] (0.100 g, 0.131 mmol) in toluene (10 ml). After stirring the reaction mixture for one hour the solvent was removed. The residue was dissolved to CH_2Cl_2 and filtered. The filtrate was concentrated and the product precipitated by addition of *n*-hexane. The red solid was washed with hexane and dried. Yield 0.128 g, 89 %. Anal. Calcd. (%) for $PtTe_2P_2C_{46}H_{36}$: C, 50.18; H, 3.30. Found: C, 49.75; H, 3.29.

Preparation of [Pt(TeTh)$_2$(*dppn*)] (3)

1.7 ml THF of solution ThTeLi (0.436 mmol), which was prepared *in situ*, was added to a suspension of [$PtCl_2$(*dppn*)] (0.110 g, 0.144 mmol) in THF (20 ml). The solution was stirred for 1.5 hours at room temperature. The solvent was then removed, the residue was dissolved in CH_2Cl_2 (25 ml) and filtered. The workup afforded a dark red crystalline solid, which was washed with *n*-hexane. Yield 0.127 g, 79 %. Anal. Calcd. (%) for $PtTe_2P_2S_2C_{42}H_{32}$: C, 45.32; H, 2.90; S, 5.76. Found C, 44.90 ; H, 3.10;S, 6.12.

Oxidative Addition Reactions of R_2Te_2 to [Pt(η²-nb)(*dppn*)]

Two series of oxidative addition reactions of $^nBu_2Te_2$, Ph_2Te_2, and Th_2Te_2 to [Pt(η²-nb)(*dppn*)] were carried out in toluene both at room temperature and at low temperature (*ca.* -80 °C). In one series, the R_2Te_2 solution (0.047 g, 0.052 g, and 0.054 g, respectively, each 0.127 mmol) in 15 mL of toluene was added dropwise to the solution of 0.100 g (0.127 mmol) [Pt(η²-nb)(*dppn*)] in 15 mL of toluene. In another series, the [Pt(η²-nb)(*dppn*)] solution [0.100 g (0.127 mmol), 15 mL toluene] was added dropwise to the R_2Te_2 solution (0.127 mmol in 15 mL toluene). The solutions were filtered and transferred into a 10 mm NMR tube, which also contained a standard of 5.0 mg of Ph_3PO.

After the recording of the NMR spectra, orange crystals were obtained in the NMR tubes of the room-temperature additions of R_2Te_2 (R = Ph, Th) to [Pt(η²-nb)(*dppn*)]. Upon determination of the crystal structures, they were found to be [Pt(TePh)(Ph)(*dppn*)] (**2**) and [Pt(TeTh)(Th)(*dppn*)] (**3**), respectively.

Computational Details

All calculations were performed with ORCA program [17] using revPBE GGA DFT functional [18] with RI approximation [19] and TZVP(-f) basis set. [20] Empirical corrections by Grimme et al. [21] have been used for dispersion forces. Solution energetics of the reactions have been taken into account using COSMO polarizable continuum model for the solvents.[22] The fundamental frequencies were calculated to assess the nature

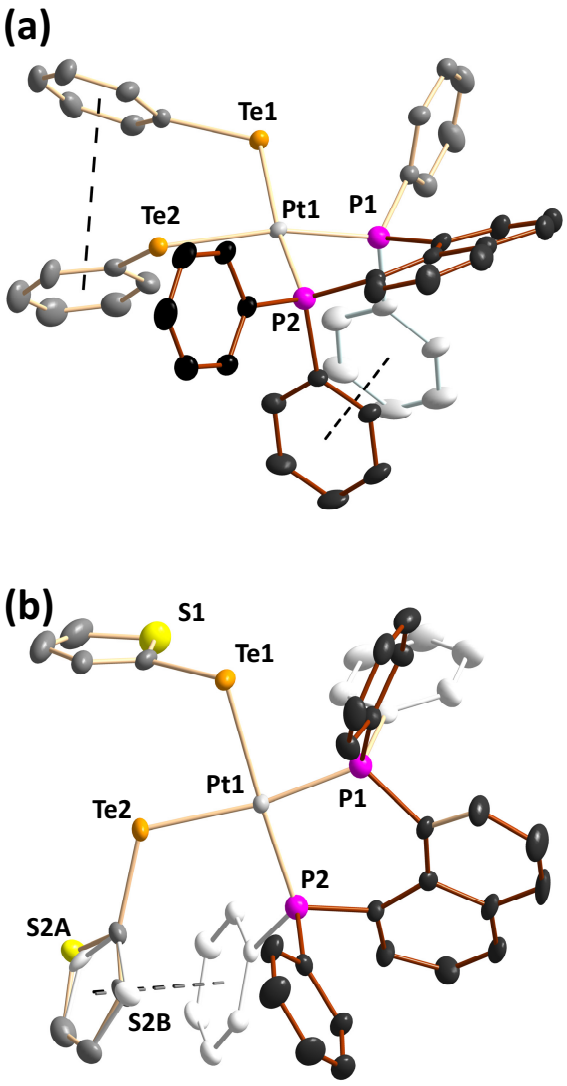

Fig. 1 Molecular structures of (a) [Pt(TePh)$_2$(*dppn*)] (**2**) and (b) [Pt(TeTh)$_2$(*dppn*)] (**3**) indicating the numbering of the atoms. The thermal ellipsoids are displayed at 50 % probability level. Hydrogen atoms have been omitted for clarity.

of stationary points and to estimate the zero-point energy (ZPE) corrections and Gibb's reaction energies. Reported transition states exhibit a single imaginary vibrational mode.

Results and discussion

General

In order to monitor the route of the oxidative addition reactions of R_2Te_2 and [Pt(η^2-nb)(*dppn*)] (R = ^{n}Bu, Ph, Th) by NMR spectroscopy, we prepared pure samples of [Pt(Te^{n}Bu)$_2$(*dppn*)] (**1**), [Pt(TePh)$_2$(*dppn*)] (**2**), and [Pt(TeTh)$_2$(*dppn*)] (**4**), and recorded their ^{31}P, ^{125}Te, and ^{195}Pt NMR spectra. The spectral interpretation was facilitated by the determination of the X-ray structures of **2**-**5**.

Preparation and Crystal structures of [Pt(TeR)$_2$(*dppn*)] [R = Ph (2), Th (3)]

[Pt(TePh)$_2$(*dppn*)] (**2**) was prepared in a good yield by reducing Ph_2Te_2 with $NaBH_4$ and reacting the resulting $PhTe^-$ with [$PtCl_2$(*dppn*)]. [Pt(TeTh)$_2$(*dppn*)] (**4**) was prepared in a similar type of ligand exchange reaction of Cl^- by $ThTe^-$, which was formed by lithiation of thiophene with ^{n}BuLi followed by the addition of tellurium.[10]

The molecular structures of **2** and **3** are shown in Fig. 1 together with the labelling of the atoms. Selected bond parameters are shown in ESI (Table 2S). In both complexes the platinum atoms show distorted square-planar coordination ($\Sigma\alpha_{Pt}$= 361.3 and 359.96 ° for **2** and **3**, respectively). The distortion is more significant in **2** than in **3** [the planes defined by the atoms Te1-Pt1-Te2 and P1-Pt1-P2 (see Fig. 1S in ESI) make an angle of 14.1 ° in **2** and 2.2 ° in **3**]. The comparison of the distortion in the related thiolato, selenolato, and tellurolato complexes is shown in Fig. 2S in ESI. In case of each chalcogen atom, the angle between the P-Pt-P and E-Pt-E planes spans a wide range. Though there are several factors governing the observed distortion, it seems that the angle between the planes increases, as the electron-withdrawing power of the organic substituent in the chalcogenolato ligand increases.

Preparation and Crystal structures of [Pt(TeR)(R)(*dppn*)] [R = Ph (4), Th (5)]

The room-temperature NMR-scale oxidative addition reactions of R_2Te_2 (R = Ph, Th) to [Pt(η^2-nb)(*dppn*)] resulted in the formation of crystals of [Pt(TePh)(Ph)(*dppn*)] (**4**) and [Pt(TeTh)(Th)(*dppn*)] (**5**) on the walls of the NMR tubes. Their molecular structures are shown in Fig. 2 together with the numbering of the atoms.

Selected bond parameters are shown in ESI (Table 2S). In both complexes **4** and **5**, platinum again shows distorted square-planar coordination ($\Sigma\alpha_{Pt}$= 360.0 and 359.0 ° for **4** and **5**, respectively). The atoms Pt1-Te1-P1-P2-C21 are almost coplanar (the angles between the planes defined by the atoms Te1-Pt1-C21 and P1-Pt1-P2 are 3.0 ° in **4** and 3.2 ° in **5**). The respective Pt-Te bond lengths of 2.6129(4) and 2.6059(5) Å in **4** and **5** are also quite normal (see discussion above), as are all other bond parameters. There is a π-stack of three aromatic rings in both complexes (see Fig. 2). In **4**, the close contacts between the phenyl rings are 3.9082(6) and 3.8783(6) Å. In case of **5**, the distance between the two thienyl rings is expectedly longer [4.2336(8) Å] than the contact between the thienyl and phenyl rings [3.8756(6) Å].

NMR Spectra of 1-5

$^{31}P\{^{1}H\}$, $^{125}Te\{^{1}H\}$ and $^{195}Pt\{^{1}H\}$ chemical shifts and $^{1}J(^{31}P\text{-}^{195}Pt)$ and $^{2}J(^{31}P\text{-}^{125}Te)$ coupling constants for complexes **1-5** are shown in Table 1. The $^{31}P\{^{1}H\}$ spectra of **1**-**3** show one singlet (-1.2, 1.0, and 2.2 ppm for **1**, **2**, and **3**, respectively) each exhibiting ^{195}Pt satellites. The chemical shifts and the $^{1}J(^{31}P\text{-}^{195}Pt)$ coupling constants of 2609-2682 Hz agree well with those in related complexes $[Pt(o\text{-}Te_2C_6H_4)(PPh_3)_2]$, *cis*-$[Pt(1,2\text{-}Te_2(C_5H_6)(PPh_3)_2]$ (2990 and 2860 Hz, respectively),[23b] $[Pt(Te_2C_5H_8O)(PPh_3)_2]$ (2906 Hz),[5c] as well as with those of $[Pt(TeR)_2(dppe)]$ (R = Ph, Th; *dppe* = diphenylphosphinoethane) (2896 and 2907 Hz, respectively),[24c] and $[Pt(Te_2C_5H_8O)(dppn)]$ (2554 Hz).[5c] The complexes **4** and **5** show two inequivalent environments for phosphorous atoms. Consequently, the $^{31}P\{^{1}H\}$ spectra showed two doublets, which both exhibit also the platinum satellites. The high-frequency resonances of **4** and **5** (10.8 and 10.9 ppm, respectively) show respective $^{1}J(^{31}P\text{-}^{195}Pt)$ coupling of 1563 and 1856 Hz, whereas the low-frequency resonances (4.0 and 3.1 ppm, respectively) exhibit $^{1}J(^{31}P\text{-}^{195}Pt)$ coupling of 2864 and 2665 Hz. Since the *trans*-influence of carbon is expected to be larger than that of tellurium, the high-frequency resonances are assigned to the phosphorus atom, which lies in *trans*-position with respect to carbon, and the low-frequency resonance is assigned to the phosphorus atom, which lies in the *trans*-position with respect to tellurium. With this assignments the $^{1}J(^{31}P\text{-}^{195}Pt)$ coupling constants are consistent with those of *cis*-[Pt(*i*-PrTe)(Ph)$(PEt_3)_2$] [1771.2 Hz (phosphorous atom *trans* to carbon atom) and 2944.1 Hz (phosphorous atom *trans* to tellurium atom].[6]

The ^{195}Pt and ^{125}Te chemical shifts, as well as the $^{1}J(^{31}P\text{-}^{195}Pt)$, $^{1}J(^{195}Pt\text{-}^{125}Te)$, and $^{2}J(^{31}P\text{-}^{125}Te)$ coupling constants of **1**-**5** are in agreement with those reported for $[Pt(Te_2C_5H_8O)(dppn)]$ (-2.3 ppm, -4955 ppm, 2554 Hz, 820 Hz, and 70 Hz respectively).[5c] ^{125}Te chemical shifts of **1**-**5** are also consistent to those of $[M(TeR)_2(dppe)]$(M = Pt, Pd, R = Ph, Th; 45-297 ppm).[24c]

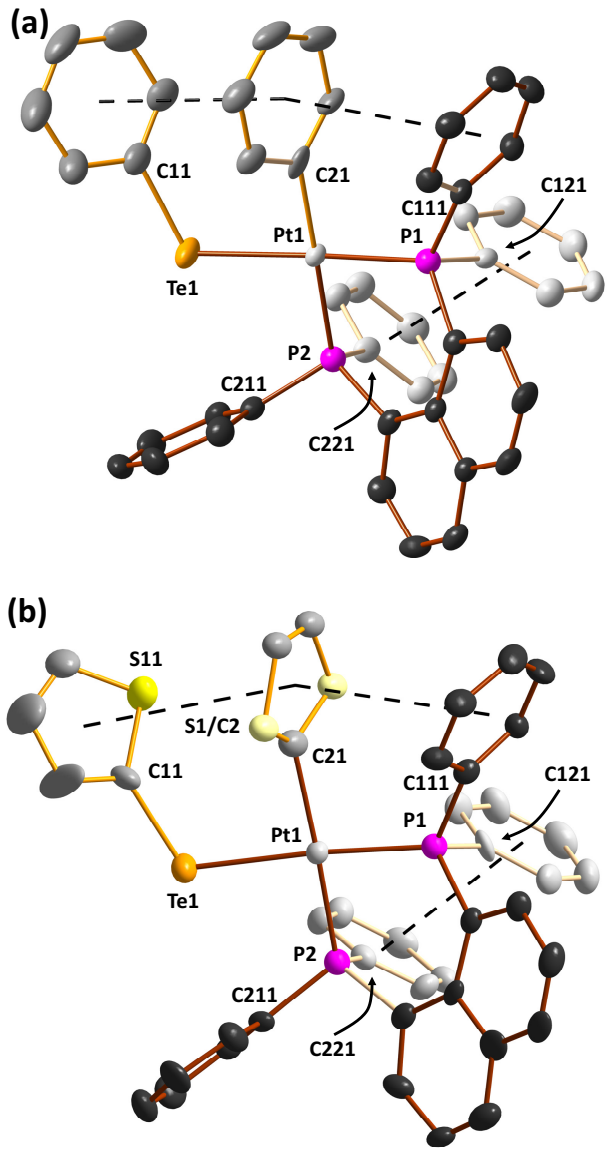

Fig.2 Molecular structures of (a) [Pt(TePh)(Ph)(*dppn*)] (**4**) and (b) [Pt(TeTh)(Th)(*dppn*)] (**5**) indicating the numbering of the atoms. The thermal ellipsoids are displayed at 50 % probability level. Hydrogen atoms have been omitted for clarity.

Oxidative addition of R_2Te_2 to Pt(0)

General. The product distribution in the oxidative addition of R_2Te_2 to Pt(0) depends both on the identity of the organic substituent of the ditelluride and on the experimental conditions. Two series of reactions were carried out: One series involved the addition of the toluene solution of R_2Te_2 to the $[Pt(\eta^2\text{-nb})(dppn)]$ solution, and the other series involved the addition of the $[Pt(\eta^2\text{-nb})(dppn)]$ solution to the R_2Te_2 solution. The reactions in each series were carried out both at room temperature and at ca. -80 °C. Whereas, most reactions involved equimolar amounts of the reactants, variations in molar ratios were also explored.

Reaction of $^{n}Bu_2Te_2$ and $[Pt(\eta^2\text{-nb})(dppn)]$. The oxidative addition of $^{n}Bu_2Te_2$ to $[Pt(\eta^2\text{-nb})(dppn)]$ solely led to the cleavage of the Te-Te bond with the formation of $[Pt(Te^{n}Bu)_2(dppn)]$ (**1**) regardless of the order of the addition of the reagents. The similar sole cleavage of the Te-Te bond has also been observed upon oxidative addition of cyclic ditelluride $OC_5H_8Te_2$ to $[Pt(\eta^2\text{-nb})(dppn)]$ with the formation of $[Pt(Te_2C_5H_8O)(dppn)]$.[5c]

Reaction of R_2Te_2 (R = Ph, Th) and $[Pt(\eta^2\text{-nb})(dppn)]$. The reactions of phenyl and thienyl ditellurides with Pt(0) are more complicated. The oxidative addition to Pt(0) led to a mixture of complexes, which indicated that the cleavage of both Te-Te and C-Te bonds takes place in the reaction. In fact, it seems that generally [Pt(TeR)(R)(*dppn*)] [R = Ph (**4**), Th (**5**)] are more abundant products in the reactions than $[Pt(TeR)_2(dppn)]$ [R = Ph (**2**), Th (**3**)]. The key question is, whether **4** and **5** are formed concurrently with **2** and **3**, respectively, or if they are produced because of the decomposition of **2** and **3**.

The reaction mixtures upon the oxidative addition of Ph_2Te_2 to $[Pt(\eta^2\text{-nb})(dppn)]$ in different conditions are shown in Fig. 3.

The addition of the Ph_2Te_2 solution to the $[Pt(\eta^2\text{-nb})(dppn)]$ solution [effective local excess of Pt(0)] at room temperature resulted in almost sole formation of [Pt(TePh)(Ph)(*dppn*)] (**4**) [see Fig. 3(a)]. The converse addition of the $[Pt(\eta^2\text{-nb})(dppn)]$ solution to the Ph_2Te_2 solution [effective local excess of

Table 1. Chemical shifts (ppm) and coupling constants (Hz) of the platinum complexes **1**-**5**.

	$^{31}P\{^{1}H\}(\delta)$	$^{125}Te\{^{1}H\}$ (δ)	$^{195}Pt\{^{1}H\}$ (δ)	$^{1}J(^{31}P\text{-}^{195}Pt)$	$^{1}J(^{125}Te\text{-}^{195}Pt)$	$^{2}J(^{31}P\text{-}^{125}Te)$	$^{2}J(^{31}P\text{-}^{31}P)$
[Pt(Te^{n}Bu)$_2$(*dppn*)] (**1**)	-1.2 (s) [a]	52 [b]	-5124(t) [b]	2609	919	67	-
[Pt(TePh)$_2$(*dppn*)] (**2**)	1.0(s) [c]	347 [b]	-5096(t) [b]	2618	590	71	-
[Pt(TeTh)$_2$(*dppn*)] (**3**)	2.2(s) [c]	185 [a]	-5057(t) [a]	2682	1058	61	-
[Pt(TePh)(Ph)(*dppn*)] (**4**)	10.8(d) [c]	386(dd) [b]	-4666(dd) [b]	1563	1105	91	38
	4.0(d) [c]			2864		131	
[Pt(TeTh)(Th)(*dppn*)] (**5**)	10.9(d) [c]	214(dd) [a]	-4657(dd) [a]	1856	1277	84	40
	3.1(d) [c]			2665		131	

[a] THF, [b] C_6D_6, the solvent was also used as a ^{2}H lock. [c] Toluene.

Ph_2Te_2] afforded approximately an equimolar mixture of [Pt(TePh)$_2$(*dppn*)] (**2**) and [Pt(TePh)(Ph)(*dppn*)] (**4**) [Fig. 3(b) and 3(c)]. The formation of **2** is favoured in case of the addition of [Pt(η^2-nb)(*dppn*)] to a stoichiometric excess of Ph_2Te_2 [Fig. 3(d) and 3(e)]. The lowering of the temperature also seems to increase the relative amount of **2** [compare Figs. 3(b) and 3(c), and Figs. 3(d) and 3(e)].

The reaction of Th_2Te_2 and [Pt(η^2-nb)(*dppn*)] proceeds in the same fashion, though the C-Te bond cleavage is more favoured than in the case of Ph_2Te_2. Even at -80 ºC, the equimolar addition of the [Pt(η^2-nb)(*dppn*)] solution to the Th_2Te_2 solution led almost solely to [Pt(TeTh)(Th)(*dppn*)] (**5**) [see Fig. 4(a)]. [Pt(TeTh)$_2$(*dppn*)] (**3**) was only observed when using a two-fold excess of Th_2Te_2 [see Fig. 4(b)].

The reaction pathways upon the oxidative addition were also investigated by revPBE GGA DFT/TZVP(-f) computations. Relative stabilities of tellurato complexes [Pt(TeR)$_2$(*dppn*)] and [Pt(TeR)(R)(*dppn*)] (R = Me, Ph, Th) were estimated using the reactions (1) and (2):

$$[Pt(\eta^2\text{-nb})(dppn)](solv) + Te_2R_2(solv) \rightleftharpoons [Pt(TeR)_2(dppn)](solv) + nb(solv) \quad (1)$$

$$[Pt(\eta^2\text{-nb})(dppn)](solv) + Te_2R_2(solv) \rightleftharpoons [Pt(TeR)(R)(dppn)](solv) + Te(s) + nb(solv) \quad (2)$$

Reaction entalpies and Gibbs energies are given in Table 2.

It is possible that tellurium in reaction (2) is involved in other, unspecified side products, which could alter the relative stabilities of [Pt(TeR)$_2$(*dppn*)] and [Pt(TeR)(R)(*dppn*)], but since NMR spectroscopic experiments provide no clear evidence for the presence of soluble side products, and the dark precipitation is observed in the reaction solutions, Te(s) is a reasonable product providing the driving force for reaction (2).

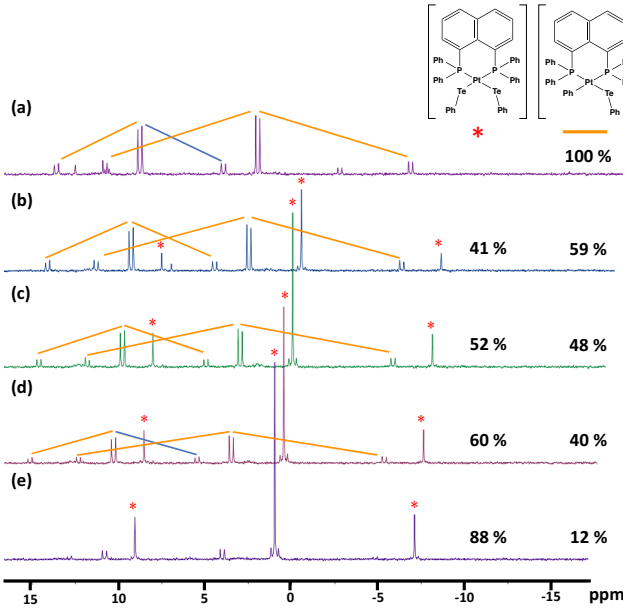

Fig. 3 Oxidative addition of Ph_2Te_2 to [Pt(η^2-nb)(*dppn*)] in toluene in different reaction conditions. (a) Ph_2Te_2 addition, RT, molar ratio 1:1. (b) [Pt(nb)(*dppn*)] addition, RT, molar ratio 1:1. (c) [Pt(nb)(*dppn*)] addition, -80 ºC, molar ratio 1:1. (d) [Pt(nb)(*dppn*)] addition to an excess of Ph_2Te_2 (molar ratio 1:2), RT. (e) [Pt(nb)(*dppn*)] addition to an excess of Ph_2Te_2 (molar ratio 1:2), -80 ºC.

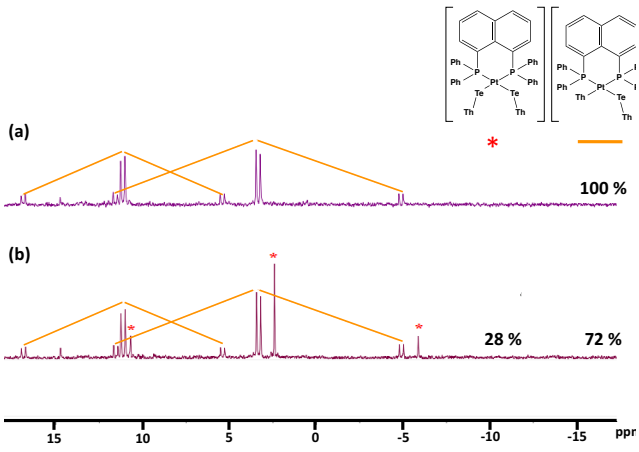

Fig. 4 Oxidative addition of Th_2Te_2 to [Pt(η^2-nb)(*dppn*)] at –80 ºC in toluene. (a) [Pt(η^2-nb)(*dppn*)] addition to an equimolar amount of Th_2Te_2. (b) [Pt(nb)(dppn)] addition of to an excess of Th_2Te_2 (molar ratio 1:2).

It can be seen from Table 2 that the calculated reaction energies suggest that both the Te-Te and Te-C bond activation becomes more favourable in the sequence Me < Ph < Th. However, [Pt(TeR)(R)(*dppn*)] becomes thermodynamically more stable with respect to [Pt(TeR)$_2$(*dppn*)] in the same sequence (Me < Ph < Th) in good agreement with the experimental observations (*vide supra*). The combination of the reactions (1) and (2) yields reaction (3):

$$[Pt(TeR)_2(dppn)](solv) \rightleftharpoons [Pt(TeR)(R)(dppn)](solv) + Te(s) \quad (3)$$

The Gibbs energies for this reaction are +1, -10, and -29 kJ mol^{-1} for ^{n}Bu, Ph, and Th, respectively (see Table 2).

Possible reaction routes from [Pt(η^2-nb)(*dppn*)] and R_2Te_2 to [Pt(TeR)$_2$(*dppn*)] and [Pt(TeR)(R)(*dppn*)] (R = alkyl group) were examined with revPBE/TZVP(-f) calculations using Me_2Te_2 as a model reagent. A suggested pathway is presented in Fig. 5.

The initial step in the oxidative addition could in principle involve either the ligand interchange through a transition state ***TS*$_{AB}$** (see Fig. 5) or by dissociation of norbornene from [Pt(η^2-nb)(*dppn*)]. The calculations clearly showed that the dissociative removal of norbornene from [Pt(η^2-nb)(*dppn*)] (Gibbs energy difference of +152.5 kJ mol^{-1}) is much higher than the interchange of ligands through the transition state [Pt(η^2-nb)(Te$_2$Me$_2$)(*dppn*)] (***TS*$_{AB}$**) in which case the activation barrier is only 47.9 kJ mol^{-1}. The removal of norbornene from ***TS*$_{AB}$** affords [Pt(*dppn*)(Te$_2$Me$_2$)] (**B**). This is reminiscent of the complex suggested by Gonzales *et al.*[9] in their study of a related oxidative addition model system [Pt(PMe$_3$)$_2$] + Te$_2$Me$_2$.

Two parallel routes are possible from **B**. The reorganization through the transition state ***TS*$_{BC}$** leads to the cleavage of the Te-Te bond and the formation of [Pt(TeMe)$_2$(*dppn*)] (**C**). The alternative pathway leads to **D** through the transition state ***TS*$_{BD}$** and subsequently to [Pt(TeMe)(Me)(*dppn*)] (**E**) due to the elimination of tellurium. The energy barrier from **B** to ***TS*$_{BD}$** is significantly higher (118.7 kJ mol^{-1}) than that from **B** to ***TS*$_{BC}$** (55.6 kJ mol^{-1}) suggesting that the formation of [Pt(TeMe)$_2$(*dppn*)] (**C**) is kinetically favoured over that of [Pt(TeMe)(Me)(*dppn*)] (**E**). This finding is consistent with the experimental observations (*vide supra*).

In addition of parallel formation of **C** and **E**, it is possible that

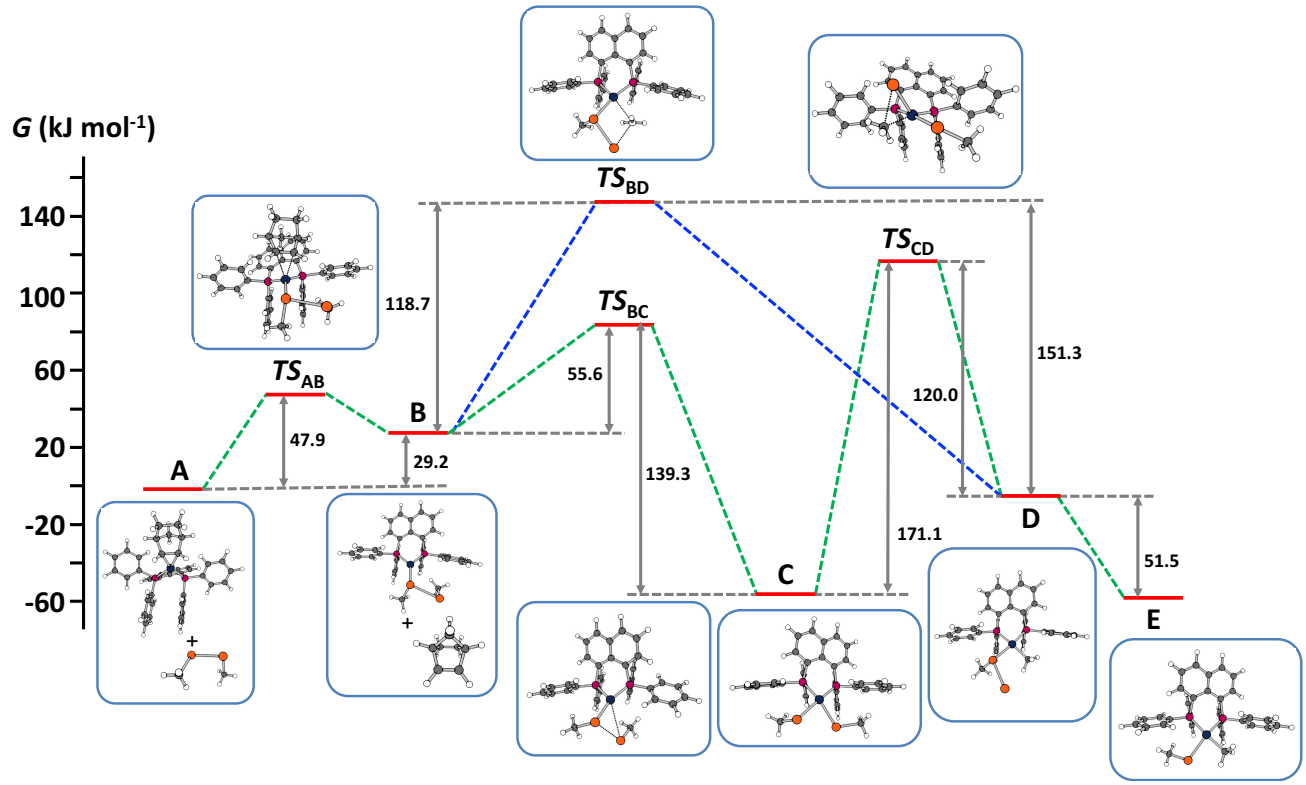

Fig. 5 Possible revPBE/TZVP(-f) energy profiles for the oxidative addition of Me_2Te_2 to [Pt(η^2-nb)(*dppn*)] according to reactions (1) and (2).

Table 2. revPBE/TZVP(-f) reaction enthalpies (ΔH) and Gibbs energies [ΔG(298 K)] of reactions (1) and (2) (R = Me, Ph, and Th) in toluene.

Reaction	ΔH/ΔG[kJ mol^{-1}] [a]		
	Me	Ph	Th
(1)	–63/–62	–102/–97	–103/–104
(2)	–63/–61	–106/–107	–130/–133
(3)	0/1	-4/-10	-27/-29

[a] Formation of Te(s) in reaction (2) has been accounted in the energy calculations using a literature value for the formation energy of Te$_2$(g) [2Te(s) ⇔ Te$_2$(g) ΔH = +168.2 kJ mol^{-1} and ΔG(298 K) = +118.0 kJ mol^{-1}] (see Fig. 3S in ESI).[26]

[Pt(TeMe)$_2$(*dppn*)] (**C**) could decompose to [Pt(TeMe)(Me)(*dppn*)] (**E**) over time, given the experimental evidence that [Pt(TeR)(R)(*dppn*)] appears to be thermodynamically more stable than [Pt(TeR)$_2$(*dppn*)]. The energy barrier of the transition state (***TS*$_{CD}$**) for this transformation, however, is even higher (171.1 kJ mol^{-1}) than that for the transition state for the direct formation of **D** from **C** and can therefore be considered very unlikely.

The calculated activation energy for the formation of the transition state ***TS*$_{BC}$** in the transformation of **B** to **C** is +55.6 kJ mol^{-1} and agrees well with that from the earlier DFT calculations at B3LYP/LANL2DZ+d level of theory for the oxidative addition model [Pt(PMe$_3$)$_2$] + Te$_2$Me$_2$ (41.4 kJ mol^{-1}).[9]

The reaction mechanism involving diaryl ditellurides seems to be more complicated. The revPBE/def2-TZVP(-f) Gibbs energies indicate (see Table 2) that with electron withdrawing organic substituents, [Pt(TeR)(R)(*dppn*)] (R = Ph, Th) lie lower in energy than [Pt(TeR)$_2$(*dppn*)], thereby explaining their facile formation. The preliminary revPBE/SVP level calculations of the route of the oxidative addition of Th$_2$Te$_2$ to [Pt(η^2-nb)(*dppn*)] indicate that the activation barriers are somewhat lower for diaryl ditellurides than for dialkyl ditellurides (see Fig. 4S in ESI), but it can be seen that this reaction pathway does not explain the strongly preferential formation of [Pt(TeR)(R)(*dppn*)] over [Pt(TeR)$_2$(*dppn*)]. Further work is currently in progress.

Since both [Pt(TePh)$_2$(*dppn*)] (**2**) and [Pt(TeTh)$_2$(*dppn*)] (**3**) can be prepared as pure crystalline products, we tested their conversion to [Pt(TeR)(R)(*dppn*)] [R = Ph (**4**), Th (**5**)] by dissolving the sample in toluene and monitoring the composition of the solution by ^{31}P NMR spectroscopy. The decomposition of neither **2** nor **3** was observed as a function of time (as exemplified for **3** in Fig. 5S in ESI). It can therefore be concluded that the formation of **4** and **5** are rather due to concurrent cleavage of the Te-Te and C-Te bonds of R$_2$Te$_2$ upon oxidative addition to the Pt(0) centre than to two consecutive processes involving the formation of **2** and **3** by oxidative addition followed by their decomposition.

Conclusions

The factors governing the oxidative addition of ^{n}Bu$_2$Te$_2$, Ph$_2$Te$_2$ and Th$_2$Te$_2$ to [Pt(η^2-nb)(*dppn*)] have been explored in this contribution. ^{n}Bu$_2$Te$_2$ reacted solely by the cleavage of the Te-Te bond with the formation of the ditellurolatoplatinum complex [Pt(Te^{n}Bu)$_2$(*dppn*)] (**1**) regardless of the order of addition of the reagents. In the case of aromatic ditellurides Ph$_2$Te$_2$ and Th$_2$Te$_2$ (Th = 2-thienyl, C$_4$H$_3$S), the reactions afforded mixtures containing in addition to [Pt(TePh)$_2$(*dppn*)] (**2**) and [Pt(TeTh)$_2$(*dppn*)] (**3**) also [Pt(TePh)(Ph)(*dppn*)] (**4**) and [Pt(TeTh)(Th)(*dppn*)] (**5**), respectively. The order of the addition of the reagents and the temperature play a significant role in the product distribution.

Addition of the toluene solution of R$_2$Te$_2$ to that of [Pt(η^2-nb)(*dppn*)] at room temperature afforded pure **4** and **5** in the case of both Ph$_2$Te$_2$ and Th$_2$Te$_2$, respectively. The reversing of the order of addition led to the formation of **2** and **4** in case of Ph$_2$Te$_2$ and **3** and **5** in case of Th$_2$Te$_2$. All reactions, which were carried out at room temperature yielded mixtures in which [Pt(TeR)(R)(*dppn*)] (**4** or **5**) was the main component. Upon lowering the temperature, the relative content of [Pt(TeR)$_2$(*dppn*)] (**2** or **3**) increased.

The DFT calculations of the reaction pathways indicated that in case of dialkyl ditellurides, the ditellurolato complexes [Pt(TeR)$_2$(*dppn*)] are the favoured end products. The activation energies for either the concurrent oxidative addition to afford [Pt(TeR)(R)(*dppn*)] or its formation by the decomposition of [Pt(TeR)$_2$(*dppn*)] are too high to be feasible. These calculations are consistent with the experimental observations.

The DFT calculations involving Th$_2$Te$_2$ indicate that in case of electron withdrawing organic groups, [Pt(TeR)(R)(*dppn*)] becomes thermodynamically more stable than [Pt(TeR)$_2$(*dppn*)]. It is likely that the reaction assumes different pathway in case of diaryl ditellurides compared to that of dialkyl ditellurides. Further exploration is currently in progress.

Acknowedgements

Financial support from Emil Aaltonen Foundation and Inorganic Materials Graduate Program are gratefully acknowledged.

References

1 (a) H. Kuniyasu, in A. Togni, and H. Grützmacher (eds.), *Catalytic Heterofunctionalization*, Wiley-VCH: Weinheim, Germany, 2001, pp. 217–251. (b) I. P. Beletskaya and C. Moberg, *Chem. Rev.,* 2006, **106**, 2320–2354. (c) I. P. Beletskaya and V. P. Ananikov, *Chem. Rev.,* 2011, **111**, 1596-1636. (d) A. Ishii, and N. Nakata, *Top. Organomet. Chem.,* 2013, **43**, 21–50. (e) A. Ogawa, *Top. Organomet. Chem.,* 2013, **43**, 325–360. (f) N. V. Orlov, *ChemistryOpen,* 2015, **4**, 682-697.

2 (a) A. Ogawa, *J. Organomet. Chem.,* 2000, **611**, 463-474. (b) V. P. Ananikov, I. P. Beletskaya, G. G. Aleksandrov and I. L. Eremenko, *Organometallics,* 2003, **22**, 1414–1421. (c) V. P. Ananikov, M. A. Kabeshov, I. P. Beletskaya, G. G. Aleksandrov and I. L. Eremenko, *J. Organomet. Chem,.* 2003, **687**, 451–461. (d) V. P. Ananikov, M. A. Kabeshov, I. P. Beletskaya, V. N. Khrustalev and M. Yu. Antipin, *Organometallics,* 2005, **24**, 1275–1283. (e) V. P. Ananikov, K. A. Gayduk, I. P. Beletskaya, V. N. Khrustalev and M. Yu. Antipin, *Chem. Eur. J.,* 2008, **14**, 2420-2434. (f) I. P. Beletskaya and V. P. Ananikov, *Eur. J. Org. Chem.*, 2007, 3431-3444.

3 (a) A. K. Singh and S. Sharma, *Coord. Chem. Rev.,* 2000*,* **209**, 49-98. (b) V. K. Jain and L. Jain, *Coord. Chem. Rev.,* 2005*,* **249**, 3075-3197. (c) V. K. Jain and L. Jain, *Coord. Chem.,* 2010, **254**, 2848-2903. (d) V. K. Jain and R. S. Chauhan, *Coord. Chem. Rev.,* 2016, **306**, 270-301.

4 (a) V. G. Albano, M. Monari, I. Orabona, A. Panunzi, G. Roviello and F. Ruffo, *Organometallics*, 2003, **22**, 1223-1230; (b) R. Oilunkaniemi, R. S. Laitinen and M. Ahlgrén, *J. Organomet. Chem.*, 2000, **595**, 232-240; (c) R. Oilunkaniemi, R. S. Laitinen and M. Ahlgrén, *J. Organomet. Chem.*, 2001, **623**, 168-175.

5 (a) H. Kuniyasu, A. Ogawa, S. L. Miyazaki, I. Ryu, N. Kambe and N. Sonoda, *J. Am. Chem. Soc.,* 1991, **113***,* 9796-9803. (b) H. Kuniyasu, A. Maruyama and A. Kurosawa,

Organometallics, 1998, **17**, 908-913. (c) A. Wagner, L. Vigo, R. Oilunkaniemi, R. S. Laitinen and W. Weigand, *Dalton Trans.,* 2008, 3535-3536.
6 L.-B. Han, N. Choi and M. Tanaka, *J. Am. Chem. Soc.,* 1997, **119**, 1795-1796.
7 L.-B. Han, S. Shimada and M. Tanaka, *J. Am. Chem. Soc.*, 1997, **119**, 8133-8134.
8 G. C. Fortman, T. Kegl, and C. D. Hoff, *Curr. Org. Chem.,* 2008, **12**, 1279-1297.
9 J. M. Gonzales, D. G. Musaeev and K. Morokuma, *Organometallics,* 2005, **24**, 4908-4914.
10 L. Engman and M. P. Cava, *Organometallics,* 1982, **1**, 470-473.
11 L. Engman and M. P. Cava, *Synth. Comm.,* 1982, **12**, 163-165.
12 R. D. Jackson, S. James, A. G. Orpen and P. G. Pringle, *J. Organomet. Chem.,* 1993, **458**, C3-C4.
13 H. Petzold, H. Görls and W. Weigand, *J. Organomet. Chem.,* 2007, **692**, 2736-2742.
14 H. C. E. McFarlane, and W. McFarlane, *J. Chem. Soc. Dalton Trans.,* 1973, 2416-2418.
15 T. G. Appleton, J. R. Hall, S. F. Ralph and C. S. Thompson, *Inorg. Chem*., 1984*,* **23**, 3521-3525.
16 G. M. Sheldrick, *Acta Crystallogr., Sect A,* 2008, **64A**, 112-122.
17 (a) The ORCA program system, version 3.0.3. (b) F. Neese, *WIREs Comput. Mol. Sci.,* 2012, **2**, 73-78
18 (a) J. P. Perdew, K. Burke and M. Ernzerhof, *Phys. Rev. Lett.,* 1996, **77**, 3865-3865. (b) Y. Zhang and W. Yang, *Phys. Rev. Lett.,* 1998, **80**, 890. (c) J. P. Perdew, K. Burke and M. Enrzernhof, *Phys. Rev. Lett.,* 1998, **80**, 891.
19 F. Neese, *J. Comput. Chem.,* 2003, **23**, 1740-1747.
20 (a) A. Schäfer, H. Horn and R. Ahlrichs, *J. Chem. Phys.,* 1992, **97**, 2571-2577. (b) F. Weigend and R. Ahlrichs, *Phys. Chem. Chem. Phys.,* 2005, **7**, 3297-3305. (c) D. Andrae, U. Häußermann, M. Dolg, H. Stoll and H. Preuß, *Theor. Chim. Acta,* 1990, **77**, 123-141.
21 (a) S. Grimme, S. Ehrlich and L. Goerigk, *J. Comput. Chem.,* 2011, **32**, 1456-1465. (b) S. Grimme, J. Antony, S. Ehrlich and H. Krieg, *J. Chem. Phys.,* 2010, **132**, 154104-19.
22 (a) A. Klamt and G. Schüürmann, *Perkin Trans. 2*, 1993, 799-805. (b) S. Sinnecker, A. Rajendran, A. Klamt, M. Diedenhofen and F. Neese, *J. Phys. Chem. A*, 2006, **110**, 2235-2245.
23 Conquest 1.19, Cambridge Crystallographic Data Center, Cambridge 2016.
24 (a) N. V. Kirij, W. Tyrra, I. Pantenburg, D. Naumann, H. Scherer, D. Naumann and Yu. L. Yagupolskii, *J. Organomet. Chem.,* 2006*,* **691**, 2679-2685. (b) D. M. Giolando, T. B. Rauchfuss and A. L. Rheingold, *Inorg. Chem.,* 1987*,* **26**, 1636-1638. (c) M. Risto, E. M. Jahr, M. S. Hannu-Kuure, R. Oilunkaniemi and R. S. Laitinen, *J. Organomet. Chem.,* 2007*,* **692**, 2193-2204. (d) R. S. Chauhan, G. Kedarnath, A. Wadawale, D. K. Maity, J. A. Golen, A. L. Rheingold and V. K. Jain, *J. Organomet. Chem.,* 2013, **737**, 40-46. (e) M. M. Karjalainen, W. Weigand, R. Oilunkaniemi and R. S. Laitinen, *Polyhedron,* 2015*,* **101**, 244-250. (f) A. A. Pasynskii, Y. V. Torubaev, A. V. Pavlova, I. V. Skabitsky, G. L. Denisov and V. A. Grinberg, *J.Cluster Sci,* 2015, **26**, 247-255.
25 (a) M. S. Hannu-Kuure, R. Oilunkaniemi, R. S. Laitinen and M. Ahlgrén, *Inorg. Chem. Commun.*, 2000, **3**, 397-399. (b) M. S. Hannu-Kuure, J. Komulainen, R. Oilunkaniemi, R. S. Laitinen, R. Suontamo and M. Ahlgrén, *J. Organomet. Chem.*, 2003, **666**, 111-120.
26 W. M. Haynes (ed.), CRC Handbook of Chemistry and Physics, 96th Ed., CSC Press, Taylor and Francis, Boca Raton 2016.